An Anisotropic Biphasic Theory of Tissue-Equivalent Mechanics: The Interplay Among Cell Traction, Fibrillar Network Deformation, Fibril Alignment, and Cell Contact Guidance

V. H. Barocas

R. T. Tranquillo

Department of Chemical Engineering and Materials Science, University of Minnesota, Minneapolis, MN 55455

We present a general mathematical theory for the mechanical interplay in tissue-equivalents (cell-populated collagen gels): Cell traction leads to compaction of the fibrillar collagen network, which for certain conditions such as a mechanical constraint or inhomogeneous cell distribution, can result in inhomogeneous compaction and consequently fibril alignment, leading to cell contact guidance, which affects the subsequent compaction. The theory accounts for the intrinsically biphasic nature of collagen gel, which is comprised of collagen network and interstitial solution. The theory also accounts for fibril alignment due to inhomogeneous network deformation, that is, anisotropic strain, and for cell alignment in response to fibril alignment. Cell alignment results in anisotropic migration and traction, as modeled by a cell orientation tensor that is a function of a fiber orientation tensor, which is defined by the network deformation tensor. Models for a variety of tissue-equivalents are shown to predict qualitatively the alignment that arises due to inhomogeneous compaction driven by cell traction.

Introduction

The mechanical interaction of motile cells with collagen fibrils[1] in the surrounding extracellular matrix is fundamental to cell behavior in soft tissues and tissue-equivalents (TEs) (highly entangled networks of collagen fibrils with entrapped cells) and thus to many biomedical problems and tissue engineering applications (Stopak and Harris, 1982; Madri and Pratt, 1986; Huang et al., 1993; L'Heureux et al., 1993; Hirai et al., 1994; Grinnell, 1994; Wilkins et al., 1994). Research using TEs of various shapes and with various mechanical constraints has led to reports of "spontaneous" development of cell alignment as compaction proceeded. Some of these reports are summarized below. All used fibroblasts unless indicated otherwise.

(A) Harris et al. (1984) reported the spontaneous development of cell aggregates in a circular TE adherent at its margins when the concentration of initially dispersed cells exceeded a threshold, with cells between aggregates oriented toward the aggregates.

(B) Klebe et al. (1989) studied TE slabs adherent at their margins (but free to compact in thickness). When the slabs were rectangular, spontaneous alignment parallel to the long axis of the rectangle was observed when the cell concentration exceeded a threshold; however, orientation remained isotropic in square slabs.

(C) Kolodney and Elson (1993) reported that cell alignment developed along the axis of a compacting TE slab that was adherent at opposite ends to fixed platens in their "isometric" cell force measurements.

(D) Grinnell and Lamke (1984) examined compacting TE hemi-ellipsoids adherent to a fixed surface at the base (shown schematically in Fig. 2(*a*) of this paper). The hemi-ellipsoids were fabricated with cells either concentrated near the free upper surface or near the adherent lower surface. In both cases, Grinnell and Lamke observed that the entire collagen network became aligned in the plane parallel to the base even though the cells did not penetrate significantly into the bulk.

(E) In the development of a dermal-equivalent, Lopez Valle et al. (1992) reported cell alignment in the plane of a compacting TE disk adherent to a fixed surface along its edge but free to compact in thickness (Fig. 3(*a*)).

(F) In the development of a media-equivalent, L'Heureux et al. (1993) reported that when a TE tube compacted around a mandrel in its lumen, thereby constraining radial compaction, but not axial compaction due to periodic disruption of adhesion with the mandrel, circumferential alignment of the smooth muscle cells developed (Fig. 4(*a*)). (It had been previously reported by Weinberg and Bell (1986) that when such tubes freely compacted, that is without mechanical constraint, the cell orientation remained essentially isotropic.) Conversely, axial cell alignment developed when adhesion of the TE tube to the mandrel eliminated axial compaction along the mandrel surface (Fig. 5(*a*)) (N. L'Heureux, personal communication).

(G) We add to this list the development of circumferential cell alignment when cells are dispersed in freely compacting TE spheres so as to be initially excluded from a core region (Fig. 6(*a*)), whereas the cell orientation remains essentially isotropic when cells are initially dispersed throughout the sphere (Barocas and Tranquillo, 1994; Bromberek et al., 1997).

These observations taken together may appear confounding with respect to the origin of cell alignment. However, the evi-

[1] Although in vivo collagen fibrils assemble to form fibers, we use "fibril" throughout this paper to refer to collagen fibers and fibrils collectively. We reserve the term "fiber" for the conceptual representation of the local network fibril in our theory.

Contributed by the Bioengineering Division for publication in the JOURNAL OF BIOMECHANICAL ENGINEERING. Manuscript received by the Bioengineering Division November 18, 1995; revised manuscript received August 26, 1996. Associate Technical Editor: R. M. Nerem.

dence summarized in the next section that cells align, exert traction, and migrate preferentially in the direction that surrounding fibrils are aligned, termed contact guidance, and that deformation of a collagen network induces alignment of its component fibrils, leads to a unifying mechanism for all of these observations: Cell traction leads to deformation of the fibrillar network, which for certain conditions such as a mechanical constraint or inhomogeneous cell distribution, can result in inhomogeneous deformations and consequent fibril alignment, leading to cell contact guidance, which affects the subsequent deformation. This interplay may govern cell accumulation in a wound and thereby its rate and extent of contraction, and be exploited to control the microstructure of bioartificial tissues and organs and thereby their functionality. The only mathematical theory proposed to account for these alignment effects (Tranquillo et al., 1992) was not generalizable to two-dimensional and three-dimensional geometries, as is the case in all of these examples except G.

We present here a general mathematical theory for this interplay that is shown to be consistent with all of the given examples above that are modeled (those that are spherically or axisymmetric, examples D–G). The theory is biphasic because it accounts for the fact that collagen gels are intrinsically two phases, collagen network and interstitial solution. It is anisotropic because it accounts for cell alignment due to fibril alignment, and fibril alignment due to inhomogeneous network deformation (anisotropic strain). The paper is organized as follows: The field equations are presented, followed by a detailed treatment of the fiber and cell orientation tensors that account for contact guidance in the field equations. After a brief discussion of the numerical methods used to solve model equations based on the theory, predictions are presented for examples D–G and compared to experimental observations (examples C and F are considered elsewhere in further detail, Barocas and Tranquillo (1997) and Barocas et al. (1997), respectively). Finally, the Discussion addresses some alternative theoretical approaches to contact guidance and some limitations of the one that we present here. A previous paper (Barocas and Tranquillo, 1994) includes our isotropic biphasic theory and a preliminary report of our anisotropic biphasic theory.

Anisotropic Biphasic Theory of Tissue-Equivalent Mechanics

The theory is based on several assumptions, which are presented below along with their justification:

- Collagen gel is comprised of two interpenetrating continuous phases: a highly entangled fibrillar network and interstitial solution (consistent with electron micrographs, e.g., Allen et al., 1984).
- The phases exhibit, generally, intraphase viscoelasticity and interphase frictional drag due to relative motion, with the (intraphase) viscosity of the solution phase being negligible (consistent with shear and compression testing (Barocas et al., 1995; Knapp et al., 1997)).
- Cells exert traction stress on the network in the direction they are oriented (consistent with polarized light micrographs of TEs, e.g., Moon and Tranquillo, 1993).
- Network fibrils (specifically, fibril segments between entanglements) reorient according to the local (macroscopic) deformation of the network (consistent with data that birefringence is induced upon TE compression and remains after stress relaxation (Girton et al., 1997)).
- Cells reorient and migrate preferentially with the preferred fiber direction (consistent with data that cell alignment is also induced upon compression and remains (Girton et al., 1997), and with cell alignment and migration measured in magnetically aligned networks (Dickinson et al., 1994)).
- All parameters except cell traction and migration, which correlate with cell spreading, are time independent (consistent with the success of the theory in predicting short-time homogeneous TE compaction (Barocas et al., 1995)); in particular, significant changes in network composition due to cell secretion are not admissible.

Biphasic theories have been used successfully in a variety of biomechanical problems, including articular cartilage (Mow et al., 1980) and arterial wall (Simon and Gaballa, 1988). We adopt the biphasic theory developed by Dembo and Harlow (1986) for cell mechanics based on the multiphase averaging theory of Drew and Segel (1971), as previously described (Barocas and Tranquillo, 1994), treating cells as a continuous component of the network phase, since they are entrapped within the network, rather than as a separate phase. Defining the average fractional volumes of network and solution as θ_n and θ_s, the excluded volume relation requires:

$$\theta_n + \theta_s = 1 \tag{1}$$

Defining the average velocities of network and solution as $\mathbf{v}_n$ and $\mathbf{v}_s$, mass conservation can be expressed in terms of volume fractions when the intrinsic phase densities are constant and nearly equal (a good approximation for protein networks and biological solutions, as Dembo and Harlow note):

$$\frac{D_n\theta_n}{Dt} = -\theta_n(\nabla \cdot \mathbf{v}_n) + R_n \tag{2}$$

$$\frac{D_s\theta_s}{Dt} = -\theta_s(\nabla \cdot \mathbf{v}_s) - R_n \tag{3}$$

where R_n is the net rate at which volume is transferred from the solution to network phase due to all reactions, and $D_i(\cdot)/Dt$ denotes the substantial derivative with respect to the velocity of phase i. The assumption that $R_n = 0$ is valid for short-term TE culture since network formation is complete before the cells begin to exert traction and there is negligible synthesis or degradation of collagen due to the cells (Nusgens et al., 1984). The sum of Eqs. (2) and (3) yields the overall incompressibility relation:

$$\nabla \cdot [\theta_n\mathbf{v}_n + \theta_s\mathbf{v}_s] = 0 \tag{4}$$

Of course, only two of the three forms of mass conservation equations are independent; we use Eqs. (2) and (4), and all subsequent substantial derivatives are with respect to $\mathbf{v}_n$.

The key result of the averaging theory of Drew and Segel as adapted by Dembo and Harlow, after omitting inertial terms, which are negligible for tissue mechanics (Odell et al., 1981), is a set of coupled mechanical force balances, which are written given our assumptions as follows:

$$\nabla \cdot [\theta_n(\boldsymbol{\sigma}_n + \tau_0 c\boldsymbol{\Omega}_c)] - \theta_n\nabla P + \varphi_0\theta_n\theta_s(\mathbf{v}_s - \mathbf{v}_n) = \mathbf{0} \tag{5}$$

$$-\theta_s\nabla P + \varphi_0\theta_n\theta_s(\mathbf{v}_n - \mathbf{v}_s) = \mathbf{0} \tag{6}$$

where $\boldsymbol{\sigma}_n$ is the stress in the network phase, P is the solution hydrostatic pressure, φ_0 is the interphase drag coefficient (inversely proportional to permeability), and $\tau_0 c\boldsymbol{\Omega}_c$ is a contractive cell traction stress assumed to act anisotropically as determined by the cell orientation tensor $\boldsymbol{\Omega}_c$ (described in the next section) with magnitude $\tau_0 c$, where c is the cell concentration. The magnitude of the cell traction stress is thus effectively bilinear in cell and network concentrations (note the term is multiplied by θ_n in Eq. (5), which weights the stress carried by the network by its local volume fraction) with τ_0 as the cell traction parameter, a measure of the intrinsic traction capacity of the cells. It may be necessary to account for inhibition of traction at high cell and network concentrations (Barocas and Tranquillo, 1994), although the bilinear form was sufficient to fit data from compacting TE spheres when a time dependence for τ_0 was included to account for cell spreading and development of traction during a lag period that precedes and overlaps

initial compaction (Barocas et al., 1995). We note that we have assumed a bilinear dependence of the interphase drag on network volume fraction by writing $\varphi_0\theta_n\theta_s$, as suggested by Dembo and Harlow (1986), although other forms are possible (e.g., Mow et al. (1986) for articular cartilage). Our confined compression studies of acellular collagen gel indicate that the assumed dependence is sufficient to describe accurately the initial compactions considered here (Knapp et al., 1996).

Equation (5) requires that a cell conservation equation be included in the theory. Fibroblasts exhibit contact guidance in noncompacting TE with magnetically aligned fibril networks (Guido and Tranquillo, 1993; Dickinson et al., 1994). These studies indicate that anisotropic migration associated with contact guidance can be modeled as an anisotropic diffusion, and that the principal direction of migration is the direction of the cell alignment (Barocas and Tranquillo, 1994). We thus propose the following:

$$\frac{Dc}{Dt} + c(\nabla \cdot \mathbf{v}_n) = \nabla \cdot (\mathcal{D}_0 \mathbf{\Omega}_c \cdot \nabla_c) + k_0 c \tag{7}$$

where $\mathcal{D}_0$ is a basal migration coefficient, and k_0 is a basal rate constant for cell division. Using a stochastic modeling treatment of cell migration (Dickinson, 1996; Dickinson and Tranquillo, 1994), it can be shown that the anisotropic diffusion is consistent with direction-independent cell speed and negligible persistence of direction as compared to speed. While a first-order rate of cell division is sufficient to model fibroblast division in freely compacting TEs (Barocas et al., 1995), this could be modified as appropriate.

Finally, Eqs. (4)–(6) can be combined to eliminate $\mathbf{v}_s$ and write the following equations in "Pressure Diffusion" form (Dembo, 1994) (the subscript n is now dropped from θ_n, $\boldsymbol{\sigma}_n$, and $\mathbf{v}_n$):

$$\nabla \cdot [\theta(\boldsymbol{\sigma} + \tau_0 c \mathbf{\Omega}_c) - P\mathbf{I}] = \mathbf{0} \tag{8}$$

$$-\nabla \cdot \left[\frac{(1-\theta)}{\theta} \nabla P \right] + \varphi_0 \nabla \cdot \mathbf{v} = 0 \tag{9}$$

We note that our biphasic theory reduces to a (pseudo-) monophasic theory (Oster et al., 1983) when permeability effects are negligible, as in the case of sufficiently small TE (Barocas and Tranquillo, 1994); in this case, there is still solution flow, but since there is no frictional loss, no pressure gradient arises (i.e., Eq. (9) is trivial).

A constitutive equation defining $\boldsymbol{\sigma}$ is motivated by the observations that in shear (Barocas et al., 1995) and confined compression (Knapp et al., 1997), on a time scale appropriate for TE experiments (i.e., hours), the collagen network can be modeled accurately as a single-relaxation time compressible upper convected Maxwell fluid (Macosko, 1994):

$$\frac{1}{2G}\overset{\nabla}{\boldsymbol{\sigma}} + \frac{1}{2\mu}\boldsymbol{\sigma} = \frac{1}{2}[\nabla \mathbf{v} + (\nabla \mathbf{v})^T] + \frac{\upsilon}{1-2\upsilon}(\nabla \cdot \mathbf{v})\mathbf{I}$$

$$\overset{\nabla}{\boldsymbol{\sigma}} \equiv \frac{D\sigma}{Dt} - \nabla \mathbf{v} \cdot \boldsymbol{\sigma} - \boldsymbol{\sigma} \cdot (\nabla \mathbf{v})^T \tag{10}$$

where $\boldsymbol{\sigma}$ is the Cauchy stress tensor, G is the shear modulus, μ is the shear viscosity, and υ is Poisson's ratio for the network.

Contact guidance is modeled by the $\mathbf{\Omega}_c$-dependent terms in Eq. (7) (anisotropic migration) and (8) (anisotropic traction). It remains to define $\mathbf{\Omega}_c$ in order make the field equations a closed system. In the following section, we describe how we relate $\mathbf{\Omega}_c$ to $\mathbf{\Omega}_f$, an orientation tensor for network fibrils, and how $\mathbf{\Omega}_f$ can be related to the network deformation field determined by the field equations presented above.

Strain-Induced Fiber Alignment and Cell Contact Guidance

As stated above, available data are consistent with contact guidance arising from cell alignment in response to aligned collagen fibrils, whether the fibril alignment is induced magnetically (with no deformation of the network) or by applied compression, the latter implying that network deformation induces the observed fibril alignment and, therefore, cell alignment. Our initial treatment of cell traction-induced fibril alignment assumes that anisotropy developing from cell traction can be modeled as if it developed from macroscopic deformation of the network. Also, anisotropic effects on viscoelasticity and permeability of the collagen network are discounted as previously described (Barocas and Tranquillo, 1994). The goal of this section is to formalize the relation between deformation and cell orientation. First, we define $\mathbf{\Omega}_f$ to characterize the orientation of the fibrils. Second, we describe how $\mathbf{\Omega}_f$ evolves with time. Finally, we relate $\mathbf{\Omega}_c$ to $\mathbf{\Omega}_f$.

Rather than attempting to model the detailed network microstructure involving the topology of long, highly entangled fibrils, we introduce the concept of a model fiber as a representation of the actual fibrillar network. Mathematically, the fiber is a unit vector that captures the fibril orientation state at a point in the network (the fiber exists at a point and occupies no volume). Since we are concerned only with fiber direction, fiber stretching is not considered. Further, the reorientation of a fiber is a function only of the local macroscopic deformation and does not depend on other fibers. The response of the cells to fibril alignment is thus modeled as a function of fiber alignment.

The orientation of a fiber with respect to a given characteristic direction can be described completely by an angle α away from the characteristic direction and an angle ϑ around the characteristic direction. The continuum assumption made in our theory implies that there is a continuous distribution of fibers at every point in space, so we consider the distribution $P(\alpha, \vartheta)$ such that the probability of finding a fiber with orientation between (α, ϑ) and $(\alpha + d\alpha, \vartheta + d\vartheta)$ is given by

$$\frac{P(\alpha, \vartheta)\sin\alpha}{2\pi} d\alpha d\vartheta, \quad \alpha \in \left[0, \frac{\pi}{2}\right], \quad \vartheta \in [0, 2\pi) \tag{11}$$

Various approaches to defining $P(\alpha, \vartheta)$ and incorporating it into models of fibrillar systems are described by Barocas and Tranquillo (1994). Based on the requirement of objectivity and the observation of birefringence during confined compression (Girton et al., 1997), we choose to define P based on the diagonalized Finger deformation tensor, $\mathbf{B} = \nabla \mathbf{u} \nabla \mathbf{u}^T$ and its associated ellipsoid (i.e., the ellipsoid whose axes have lengths equal to the eigenvalues of $\mathbf{B}$ and directions defined by the eigenvectors of $\mathbf{B}$). We define the probability of finding a fiber at an orientation (α, ϑ) to be proportional to the differential surface area of the ellipsoid at that position. Mathematically, this is expressed by

$$P(\alpha, \vartheta)\sin\alpha = \frac{r}{A}\sqrt{\left(\frac{\partial r}{\partial \vartheta}\right)^2 + \left(\frac{\partial r}{\partial \alpha}\right)^2 \sin^2\alpha + r^2 \sin^2\alpha}$$

$$\approx \frac{r^2(\alpha, \vartheta)\sin\alpha}{A} \tag{12}$$

where $r(\alpha, \vartheta)$ is the radius of the ellipsoid at angles α and ϑ, and A is a normalization factor proportional to the total surface area of the ellipsoid. For small strains, the ellipsoid approaches a sphere, and the partial derivatives approach zero; this leads to the approximate form in Eq. (12), which was used in Barocas and Tranquillo (1994) for analyzing small deformations of TE spheres. In the case of isotropic strain, $r(\alpha, \vartheta)$ is a constant, and $P(\alpha, \vartheta)$ is identically 1. The use of a probability distribution

based on the deformation ellipsoid has the important advantage that no new parameters are introduced, since the alignment is determined by the macroscopic deformation. Also, this approach extends readily to networks that have been preoriented by manipulation of the gelation environment (e.g., magnetic alignment (Tranquillo et al., 1995; Barocas et al., 1997)). We therefore choose to use this deformation-based distribution as a preliminary model of fiber alignment.

Rather than use P directly in the field equations, it is convenient to introduce it through a fiber orientation tensor, Ω_f, defined by

$$\Omega_f \equiv 3 \int_0^{\pi/2} \int_0^{2\pi} \mathbf{r}(\alpha, \vartheta) \otimes \mathbf{r}(\alpha, \vartheta) \frac{P(\alpha, \vartheta) \sin \alpha}{2\pi} d\vartheta d\alpha \tag{13}$$

where $\mathbf{r}$ is the unit vector in the direction of a fiber, and the symbol $\otimes$ denotes dyad product. This is a continuous analog of the discrete definition of the orientation tensor by Farquhar et al. (1990). The factor 3 ensures that $\Omega_f = \mathbf{I}$ when the network is isotropic (rather than having tr $\Omega_f = 1$). The relative alignment of the fibers in the direction of an arbitrary unit vector $\mathbf{v}$ is defined by $(\mathbf{v} \cdot \Omega_f \cdot \mathbf{v})$, with a value greater than one indicating that the direction of $\mathbf{v}$ is preferentially oriented in the direction of aligned fibers. The derivation of specific components of Ω_f from Eqs. (12) and (13) is described in the appendix. Since tr $\Omega_f = 3$, we know that the diagonal components of Ω_f must range from 0 (no orientation in a given direction) to 3 (uniaxial alignment). Off-diagonal terms of Ω_f are non-zero when the principal axes of orientation are not coincident with the coordinate axes. Figure 1 shows some possible fiber distributions and the associated values of Ω_f.

The observation that cells align with respect to the same principal axis as the fibrils, along with the constraint that the cells are isotropically oriented when the fibrils are so oriented, suggest that the cell orientation tensor, Ω_c be written as a monotonically increasing function of the fiber orientation tensor, Ω_f, for example

$$\Omega_c = \frac{3}{\text{tr } (\Omega_f)^\kappa} (\Omega_f)^\kappa \tag{14}$$

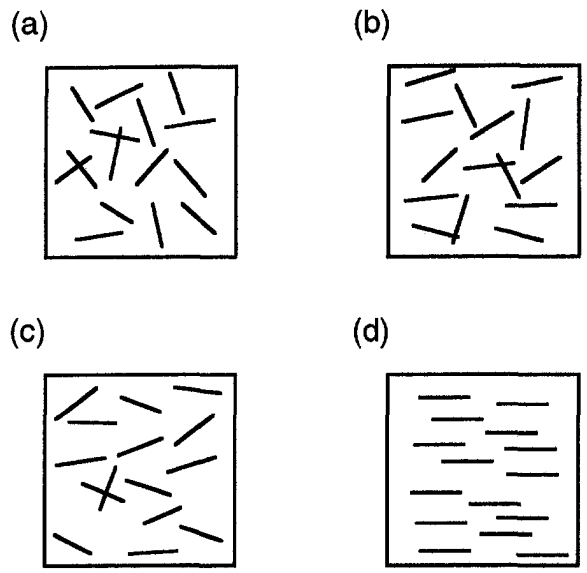

Fig. 1 Sample orientation distributions and the resulting orientation tensor Ω_f: The four boxes correspond to different principal values of the orientation tensor. Taking the out-of-plane elements of Ω_f to be zero to simplify visualization, the in-plane components of Ω_f are (*a*) [1.5, 1.5], (*b*) [2.0, 1.0], (*c*) [2.5, 0.5], (*d*) [3.0, 0.0].

Our recent studies on confined compression of TEs (Girton et al., 1997) indicate that Eq. (14) provides an accurate fit, and that $\kappa \approx 4$ for both fibroblasts and smooth muscle cells, i.e., cell alignment is generally more pronounced than fibril alignment.

Solution of Field Equations

In order to use the anisotropic biphasic theory, we must solve the system of integro-partial differential equations (I-PDEs). Since the equation set does not admit a general analytical solution, we compute numerical solutions. The spatial derivatives are discretized using a mixed finite element method, converting the I-PDE system into a differential-algebraic equation (DAE) system. The important features of the solution method for axisymmetric problems are given below; further details are described elsewhere (Barocas and Tranquillo, 1997). Because we are interested in relatively small transient deformations, it is convenient to solve the problem in a Lagrangian (material) reference frame moving with the network phase. For the small deformations of interest here, no remeshing is necessary, although remeshing would be possible for larger deformations (see, for example, Dembo (1994)). Our mixed formulation uses piecewise bilinear basis functions for the pressure, piecewise biquadratic basis functions for the velocity, cell concentration, and network volume fraction, and discontinuous (nonconforming) piecewise biquadratic basis functions for network stress. The discontinuous basis functions for stress can be introduced easily because gradients of stress do not appear in the weak form, and in fact these basis functions are central to achieving a stable solution.

The resulting DAE problem is solved using the DASPK subroutine, a variable order, variable time step Euler–Crank DAE solver (Brown et al., 1994). DASPK has the advantage over previous DASSL subroutines (such as DASRT used by Barocas and Tranquillo (1994)) of using the preconditioned GMRES iterative method (Saad and Schultz, 1986) to solve the linear problem associated with the Newton iteration necessary at each time step. For the axisymmetric problem, the iterative solution is far more efficient then the band solver used by the earlier DASSL routines. We use a preconditioner based on Dembo's "Pressure Diffusion" algorithm (Dembo, 1994).

Simulation of Spontaneous Contact Guidance Observed in Tissue-Equivalents

Toward a validation of our general theory, we present here comparisons between published observations and model predictions based on our theory for the radially and spherically symmetric TE systems (D–G) described in the introduction. We used parameter estimates for the collagen network properties based on a confined compression study (Knapp et al., 1997): $G = 1.5 \times 10^4$ dyn/cm^2, $\mu = 1.1 \times 10^8$ dyn·s/cm^2, $\varphi_0 = 4.2 \times 10^6$ dyn·s/cm^4. Based on Barocas et al. (1995) and the confined compression data, we took $\tau_0 = 0.014$ dyn·cm/cell and $k_0 = 5.3 \times 10^{-6}$ s^{-1}, and based on Dickinson et al. (1994), we took $\mathcal{D}_0 = 1.7 \times 10^{-10}$ cm^2/s. (Cell division and migration are both relatively unimportant events for these parameter values.) The geometry of the confined compression test does not allow separation of υ from G and μ, so we have assumed $\upsilon = 0.2$, a value reported for inorganic gels (Scherer, 1989a). For the purpose of illustration, we performed all of the simulations presented here with $\kappa = 1$, which implies that $\Omega_c = \Omega_f$. As a result, the subscripts "c" and "f" are unnecessary and are omitted in the results.

For each TE system, we show a schematic describing the problem geometry and the boundary conditions used. The shading marks the region that is simulated after accounting for inherent symmetries. The boundary conditions fall into four basic categories depending on the type of boundary ("n" and "t" refer to normal and tangent to the boundary):

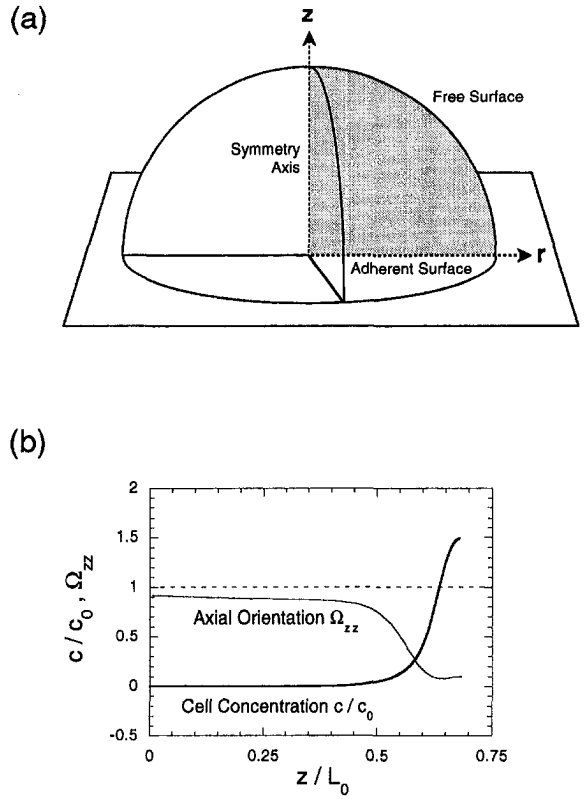

Fig. 2 Adherent TE hemi-ellipsoids (cf. Grinnell and Lamke (1984)): (*a*) The hemi-ellipsoid is attached at the base, is axisymmetric, and has a free surface. (*b*) The predicted cell concentration and orientation along the *z* axis after 20 h (the subscript "0" denotes initial value). The cells have not penetrated the bulk of the sample, but fibers throughout the entire sample exhibit alignment parallel to the base ($\Omega_{zz} < 1$).

- *Free:* These are boundaries exposed to the surrounding tissue culture medium. Since there is no significant surface tension in the network, we assume $P = (\boldsymbol{\sigma} + \tau_0 c \boldsymbol{\Omega}_c)_{nn} = (\boldsymbol{\sigma} + \tau_0 c \boldsymbol{\Omega}_c)_{nt} = 0$. We assume there is no cell migration across the edge of the network, so we take $\partial c/\partial n = 0$.
- *Adherent:* These boundaries represent surfaces to which the network adheres, implying no slip ($v_t = 0$) and no penetration ($v_n = 0$). Although it is not necessary that such a surface also be impermeable, all adherent surfaces studied here are impermeable, implying that $\partial c/\partial n = \partial P/\partial n = 0$.
- *Symmetry:* These boundaries are planes, axes, or points of symmetry. Because of symmetry, we have $v_n = (\boldsymbol{\sigma} + \tau_0 c \boldsymbol{\Omega}_c)_{nt} = 0$, and $\partial c/\partial n = \partial P/\partial n = 0$.
- *Free-Slip:* This is the boundary condition on a nonadherent mandrel used in the media-equivalent fabrication. It is equivalent to the symmetry boundary condition.

Adherent TE Hemi-ellipsoids

The TE system of Grinnell and Lamke (1984) is shown schematically in Fig. 2(*a*). A hemi-ellipsoid was formed by allowing a drop of collagen solution to gel on an adhesive substratum and then adding fibroblast-containing medium, allowing the cells to settle on the top (free) surface of the gel. (We have not simulated the companion experiment in which cells were located primarily on the bottom of the hemi-ellipsoid.) Two key observations were made regarding the reorientation of the initially isotropic network. First, the collagen fibrils and the cells near the surface showed alignment in the plane parallel to the substratum, which is expressible in our formulation as $\Omega_{zz} < 1$ (Ω_{rr}, $\Omega_{\theta\theta} > 1$); second, this alignment was observed for fibrils throughout the sample even though there was relatively little cell migration away from the surface.

We simulated their TE hemi-ellipsoids using an initial cell distribution that was quadratic near the free surface and zero in the bulk. Figure 2(*b*) shows that the simulation agrees qualitatively with the experimental observations. The plot shows the predicted cell concentration and axial (Ω_{zz}) orientation measured along the z axis after 20 h of simulated experiment. We see that the cells do not penetrate significantly into the bulk of the sample ($c \approx 0$ for $z < 0.7\ L_0$). In contrast, alignment of the fibers in the plane parallel to the substratum, indicated by $\Omega_{zz} < 1$, occurs for all values of z.

Adherent TE Disks

The next TE system we studied was the dermal-equivalent of Lopez Valle et al. (1992), shown in Fig. 3(*a*). In this system, a TE disk was allowed to compact axially, but the outer edge was attached to a ring so that no radial compaction was possible. The investigators reported that both cells and collagen fibrils exhibited radial and circumferential rather than axial orientation, which is expressed as $\Omega_{\theta\theta}$, $\Omega_{rr} > 1$, $\Omega_{zz} < 1$.

Again, the model shows qualitative agreement with experiment. We predict a steady increase in radial and circumferential versus axial orientation during the course of an experiment, shown in Fig. 3(*b*). We note that Lopez Valle et al. made a number of observations (e.g., phenotypic modification of the fibroblasts and folding of the surface of free-floating TE disks) that are beyond the scope of the current theory; the theory, when used to model a free-floating TE disk, predicts homogeneous, isotropic compaction. The orientation behavior of the disk constrained at the outer edge, however, is predicted well using the theory.

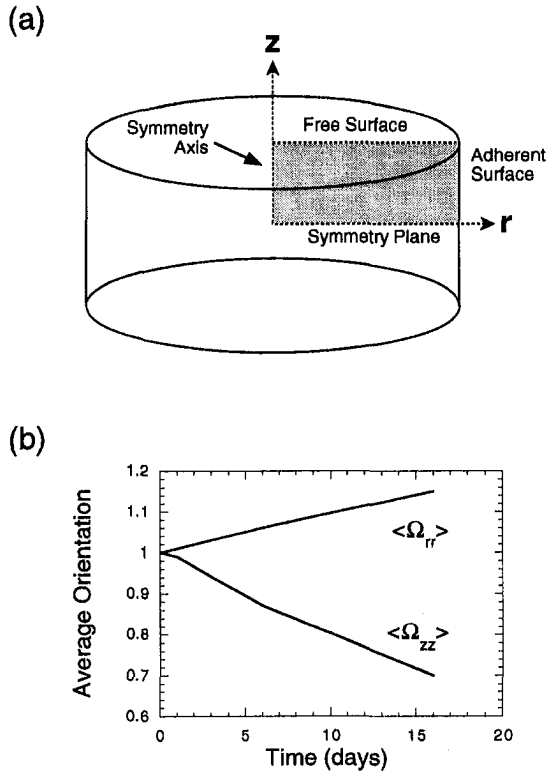

Fig. 3 Adherent TE disks (cf. Lopez Valle et al. (1992)): (*a*) The axisymmetric disk is allowed to compact axially, but the outer edge is attached to an adherent surface. (*b*) The model predicts an equal increase in radial and circumferential alignment and a decrease in axial alignment ($\Omega_{\theta\theta} = \Omega_{rr} > 1$, $\Omega_{zz} < 1$). The angular brackets denote domain-averaged values at a particular simulation time.

Adherent and Nonadherent TE Tubes

There has been considerable recent research aimed toward the fabrication of a bioartificial artery. The medial layer is made from a collagen gel tube seeded with smooth muscle cells, resulting in significant compaction of the media-equivalent (L'Heureux et al., 1993; Hirai et al., 1994; Tranquillo et al., 1995). The anisotropic biphasic theory offers the opportunity for significant advances in media-equivalent design because circumferential alignment of the collagen fibrils and smooth muscle cells as in the native arterial media is desirable (possibly conferring the requisite properties). We discuss here two examples of alignment developed during TE tube compaction: the effect of a nonadherent mandrel constraining radial compaction (Fig. 4(a)), and the effect of an adherent mandrel eliminating axial compaction (Fig. 5(a)). A more detailed analysis of the former is presented elsewhere (Barocas et al., 1997).

L'Heureux et al. (1993) reported that when adhesion of the TE tube to the mandrel was periodically disrupted, circumferential alignment of the fibrils and cells was predominantly observed. Further, they report that slip along the mandrel was necessary to obtain the desired alignment. As shown in Fig. 4(b), we predict a significant increase in circumferential alignment ($\Omega_{\theta\theta} > 1$) during the compaction of the TE tube around a nonadherent mandrel, in agreement with the experimental observation. In contrast, axial alignment predominates if adhesion is not disrupted (N. L'Heureux, personal communication). Figure 5(b) shows that the simulation predicts some increase in circumferential alignment (although less than that predicted for the free-slip case, Fig. 4(b)), but significantly more alignment in the axial direction ($\Omega_{zz} > \Omega_{\theta\theta} > 1$). These predictions are all in qualitative agreement with the experimental observations.

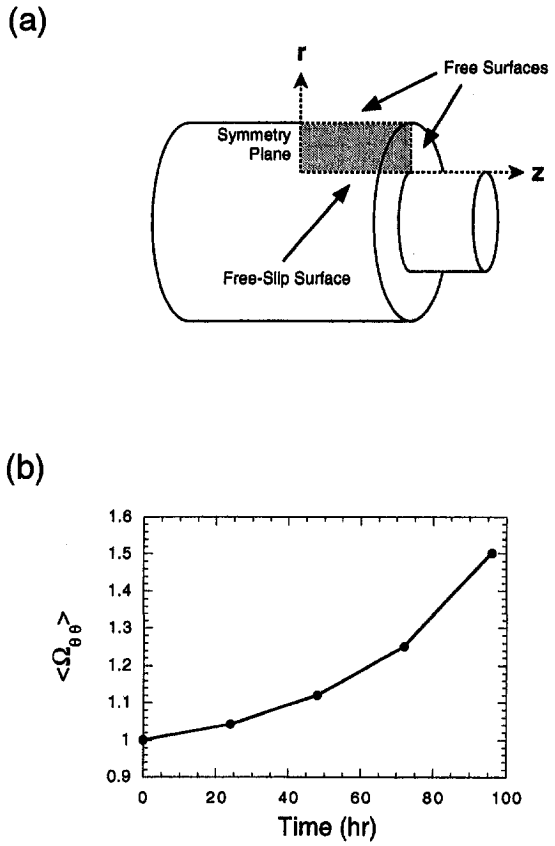

Fig. 4 TE tubes with free-slip mandrel (cf. L'Heureux et al. (1993)): (*a*) The circumference and ends of the axisymmetric tube are free surfaces; the central mandrel is impenetrable and impermeable, but there is no shear stress along it (free slip surface). (*b*) The model predicts an increase in circumferential alignment ($\Omega_{\theta\theta} > 1$).

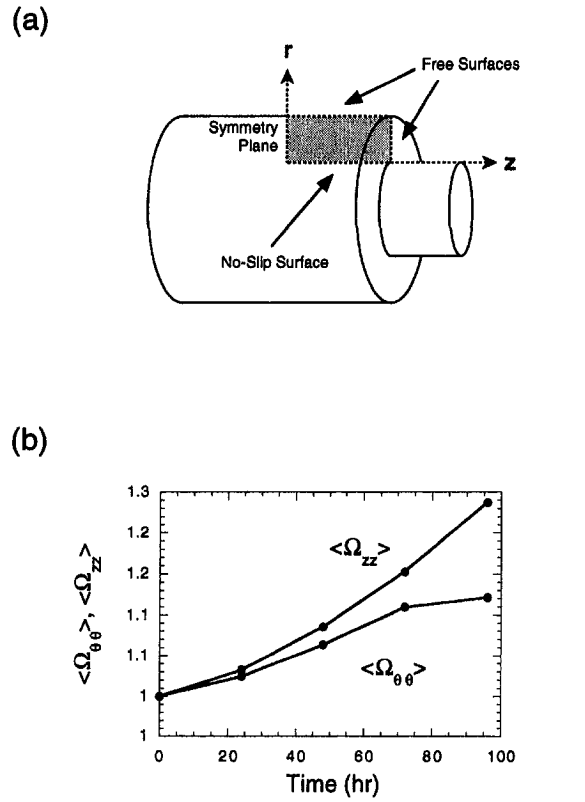

Fig. 5 TE tubes with adherent mandrel (cf. L'Heureux et al. (1993)): (*a*) The system is identical to Fig. 4 except that the mandrel exhibits no slip. (*b*) The elimination of axial compaction leads to an increase in axial alignment ($\Omega_{zz} > 1$) and inhibits the increase in circumferential alignment relative to the free-slip mandrel case.

Floating TE Spheres

The fibroblast-populated microsphere (FPM) wound assay, shown schematically in Fig. 6(a), consists of continuous sphere of fibrin gel whose core is initially cell-free (representing the wound site) and whose surrounding shell initially contains a homogeneous fibroblast distribution (representing undamaged tissue surrounding the wound site). (Fibrin gels resemble collagen gels in every aspect discussed herein, so our theory applies.) The sphere is then placed in the medium and floats during compaction. The appropriate boundary conditions are thus a free surface at the sphere surface and symmetry at the sphere origin. It is observed that as compaction proceeds, a marked circumferential alignment of the cells in the shell develops while little cell invasion of the core occurs. Figure 6(b) shows that when cells are initially excluded from the core, consistent with the FPM wound assay, the model predicts the observed circumferential alignment ($\Omega_{\theta\theta} > 1$). Due to the transverse isotropy of the system ($\Omega_{\phi\phi} = \Omega_{\theta\theta}$), the maximum possible $\Omega_{\theta\theta}$ value is 1.5, but the predicted alignment is less pronounced than in the other TE systems examined. This can be explained by the fact that a rigid constraint is involved in the other systems, whereas the cell-free fibrin gel core, which acts as a constraint on compaction in the FPM wound assay, is deformable. Interestingly, it is also observed that if the cells are initally present in the core but excluded from the shell, a marked radial alignment develops with little invasion of the shell. Figure 6(b) shows that the model predicts the observed radial alignment ($\Omega_{\theta\theta} < 1$) as well. (The model predicts homogeneous compaction, and consequently no alignment ($\boldsymbol{\Omega} = \mathbf{I}$), for the case when cells are initially dispersed throughout the sphere, however, which is also observed.)

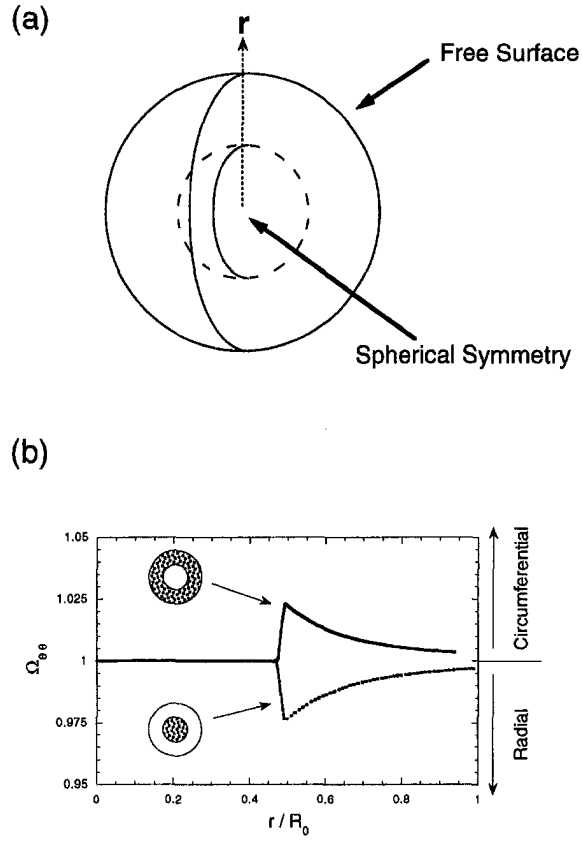

Fig. 6 Nonadherent TE sphere: (*a*) In the FPM wound assay, cells are initially distributed homogeneously throughout the outer shell of the floating sphere, but the core is initially cell-free. (*b*) The model predicts the development of circumferential alignment ($\Omega_{\theta\theta} > 1$), particularly in the region just outside the core. If cells are placed only in the core, the model predicts radial alignment ($\Omega_{rr} < 1$).

Discussion

We have used an anisotropic biphasic theory to describe the mechanics of TEs. The theory accounts for fibril alignment, associated with inhomogeneous network deformation driven by cell traction, and the resulting cell contact guidance, allowing us to predict observations in a variety of in vitro experiments. With appropriate modifications, this theory may be valid for relevant physiological processes, such as wound contraction (Tranquillo and Barocas, 1996).

Syneresis can be modeled as a change in the stress-free state of a gel leading to an apparent strain rate (Scherer, 1989b). This approach could be incorporated into our biphasic theory by replacing the traction stress term with an analogous strain rate term. For the simple situation of the FPM assays, the two approaches yield similar results (Barocas et al., 1995), but for more complex ones such as adherent TEs, they yield very different results. Notably, a strain rate theory cannot predict the partial recovery of a compacted TE when the cells are lysed (Guidry and Grinnell, 1985). Thus, for TEs, we conclude that the incorporation of cell traction as a stress is preferred.

Just as the compaction can be treated as a stress-based or a strain-based process, so can the reorientation of the fibrils. In externally loaded systems, such as cartilage or fiber reinforced composites, it is common to predict fiber reorientation based on the strain field (Farquhar et al., 1990; Schwartz et al., 1994), and we have presented here a simple method for predicting fibril reorientation based on the strain in the collagen network. It has been proposed that actin filament reorientation in cytogel can be predicted based on anisotropic stress rather than strain (Sherratt and Lewis, 1993); because their model treats cytogel as an elastic medium, stress and strain are equivalent. Since collagen gel is a viscoelastic fluid, stress relaxes to zero over time in the absence of a stress source; a stress-based theory would then require that the network return to isotropy after lysing the cells. The observation that alignment in a compacted TE remains after the cells are lysed (Guidry and Grinnell, 1985) is thus consistent with a strain-based theory and not a stress-based theory.

The anisotropic biphasic theory has been used to describe a variety of TE systems in which alignment arises through inhomogeneous cell traction-driven deformation. The model predictions have shown qualitative agreement with observations in all cases, but the fundamental assumption that cells align according to the macroscopic strain field, while leading to predictions consistent with all the TE systems examined, may not always be valid. For example, cell alignment may result from other signals beside fibril alignment in an oscillatory strain field or be influenced by the local alignment of fibrils around neighboring cells for TEs with high cell concentrations. Further, cell migration may not be accurately modeled by the form of anisotropic diffusion as proposed in Eq. (7) given its associated assumptions and absence of validating cell tracking data for contact guidance in a gradient of fibril alignment. However, the manifestation of contact guidance in a TE as anisotropic migration is negligible as compared to anisotropic traction based on the estimated value of $\mathcal{D}_0$ in TEs of uniform alignment in which cell tracking was performed. The prediction that negligible cell migration is occurring on the time scale of significant TE compaction is consistent with time-lapse video microscopy observations of the floating TE spheres (Bromberek et al., 1997).

Acknowledgments

The analysis by Mihir Wagle of contact guidance as an anisotropic diffusion based on the model of Dickinson (1996) is gratefully acknowledged. This work has been supported by an NIH FIRST Award to RTT (R29-GM46052). A grant from the Minnesota Supercomputer Institute to RTT is acknowledged.

References

Allen, T. D., S. L. Schor and A. M. Schor, 1984, "An ultrastructural review of collagen gels, a model system for cell-matrix, cell-basement membrane and cell-cell interactions," *Scan. Electron. Microsc.*, Vol. 1, pp. 375–390.

Barocas, V. H., and R. T. Tranquillo, 1994, "Biphasic theory and in vitro assays of cell-fibril mechanical interactions in tissue-equivalent collagen gels," in: *Cell Mechanics and Cellular Engineering*, Mow, V. C., Guilak, F., Tran-Son-Tay, R., and Hochmuth, R. M. eds., Springer-Verlag, New York, pp. 185–209.

Barocas, V. H., A. G. Moon, and R. T. Tranquillo, 1995, "The fibroblast-populated collagen microsphere assay of cell traction force—Part 2. Measurement of the cell traction parameter," ASME JOURNAL OF BIOMECHANICAL ENGINEERING, Vol. 117, pp. 161–170.

Barocas, V. H., and R. T. Tranquillo, 1997, "A finite element solution for the anisotropic biphasic theory of tissue-equivalent mechanics: the effect of contact guidance on isometric cell traction measurement," ASME JOURNAL OF BIOMECHANICAL ENGINEERING, accepted.

Barocas, V. H., T. S. Girton, and R. T. Tranquillo, 1997, "Engineered alignment in media-equivalents: magnetic prealignment and mandrel compaction," ASME JOURNAL OF BIOMECHANICAL ENGINEERING, submitted.

Bromberek, B. A., V. H. Barocas, and R. T. Tranquillo, 1997, "A novel in vitro wound healing and contraction assay," in preparation.

Brown, P. N., A. C. Hindmarsh, and L. R. Petzold, 1994, "Using Krylov methods in the solution of large-scale differential-algebraic systems," *SIAM J. Sci. Comp.*, Vol. 15, pp. 1467–1488.

Dembo, M., 1994, "Continuum Theories of Cytoskeletal Mechanics: Solution by a finite element method," Los Alamos National Laboratory Unclassified Report #94-3454.

Dembo, M., and F. Harlow, 1986, "Cell motion, contractile networks, and the physics of interpenetrating reactive flow," *Biophys J.*, Vol. 50 (1), pp. 109–121.

Dickinson, R. B., S. Guido, and R. T. Tranquillo, 1994, "Biased cell migration of fibroblasts exhibiting contact guidance in oriented collagen gels," *Ann. Biomed. Eng.*, Vol. 22 (4), pp. 342–356.

Dickinson, R. B., 1996, "A model for cell migration by contact guidance," in: *Dynamics of Cell and Tissue Motion*, Alt, W., A. Deutsch, and G. A. Dunn, eds., Birkhauser Verlag, Basel.

Drew, D. A., and L. A. Segel, 1971, "Averaged equations for two-phase flows," *Studies Appl. Math.*, Vol. 1 (3), pp. 205–231.

Farquhar, T., P. R. Dawson, and P. A. Torzilli, 1990, "A microstructural model for the anisotropic drained stiffness of articular cartilage," ASME JOURNAL OF BIOMECHANICAL ENGINEERING, Vol. 112, pp. 414–425.

Girton, T. S., V. H. Barocas, and R. T. Tranquillo, 1997, "Reorientation and alignment of collagen fibrils and tissue cells in confined conmpression of a tissue-equivalent," in preparation.

Grinnell, F., and C. R. Lamke, 1984, "Reorganization of hydrated collagen lattices by human skin fibroblasts," *J. Cell Sci.*, Vol. 66, pp. 51–63.

Grinnell, F., 1994, "Fibroblasts, myofibroblasts, and wound contraction," *J. Cell Biol.*, Vol. 124 (4), pp. 401–4.

Guido, S., and R. T. Tranquillo, 1993, "A methodology for the systematic and quantitative study of cell contact guidance in oriented collagen gels: Correlation of fibroblast orientation and gel birefringence," *J. Cell Sci.*, Vol. 105, pp. 317–331.

Guidry, C., and F. Grinnell, 1985, "Studies on the mechanism of hydrated collagen gel reorganization by human skin fibroblasts," *J. Cell Sci.*, Vol. 79, pp. 67–81.

Harris, A. K., D. Stopak, and P. Warner, 1984, "Generation of spatially periodic patterns by a mechanical instability: a mechanical alternative to the Turing model," *J. Embryol. Exp. Morphol.*, Vol. 80, pp. 1–20.

Hirai, J., K. Kanda, T. Oka, and T. Matsuda, 1994, "Highly oriented, tubular hybrid vascular tissue for a low pressure circulatory system," *ASAIO J.*, Vol. 40, pp. M383–388.

Huang, D., T. R. Chang, A. Aggarwal, R. C. Lee, and H. P. Ehrlich, 1993, "Mechanisms and dynamics of mechanical strengthening in ligament-equivalent fibroblast-populated collagen matrices," *Ann. Biomed. Eng.*, Vol. 22 (3), pp. 289–305.

Klebe, R. J., Caldwell, H., and Milam, S., 1989, "Cells transmit spatial information by orienting collagen fibers," *Matrix*, Vol. 9, pp. 451–458.

Knapp, D. M., V. H. Barocas, and R. T. Tranquillo, 1996, "Rheology of reconstituted type I collagen gel in confined compression," *J. Rheol.*, submitted.

Kolodney, M. S., and E. L. Elson, 1993, "Correlation of myosin light chain phosphorylation with isometric contraction of fibroblasts," *J. Biol. Chem.*, Vol. 268 (32), pp. 23850–23855.

L'Heureux, N., L. Germain, R. Labbe, and F. A. Auger, 1993, "In vitro construction of a human blood vessel from cultured vascular cells: a morphologic study," *J. Vasc. Surg.*, Vol. 17 (3), pp. 499–509.

Lopez Valle, C. A., F. A. Auger, R. Rompre, V. Bouvard, and L. Germain, 1992, "Peripheral anchorage of dermal equivalents," *Br. J. Dermatology*, Vol. 127, pp. 365–371.

Macosko, C. W., 1994, *Rheology: Principles, Measurements, and Applications*, VCH, New York.

Madri, J. A., and B. M. Pratt, 1986, "Endothelial cell-matrix interactions: in vitro models of angiogenesis," *J. Histochem. Cytochem.*, Vol. 34 (1), pp. 85–91.

Moon, A. G., and R. T. Tranquillo, 1993, "The fibroblast-populated collagen microsphere assay of cell traction force—Part 1. Continuum Model," *AIChE J.*, Vol. 39, pp. 163–177.

Mow, V. C., S. C. Kuei, W. M. Lai, and C. G. Armstrong, 1980, "Biphasic creep and stress relaxation of articular cartilage in compression: theory and experiments," ASME JOURNAL OF BIOMECHANICAL ENGINEERING, Vol. 102, pp. 73–84.

Mow, V. C., M. K. Kwan, W. M. Lai, and M. H. Holmes, 1986, "A finite deformation theory for nonlinearly permeable soft hydrated biological tissues," in: *Frontiers in Biomechanics*, Schmid-Schonbein, G. W., Woo, S. L.-Y., and Zweifach, B. W., eds., Springer-Verlag, New York, pp. 153–179.

Nusgens, B., C. Merrill, C. Lapiere, and E. Bell, 1984, "Collagen biosynthesis by cells in a tissue equivalent matrix in vitro," *Coll. Relat. Res.*, Vol. 4 (5), pp. 351–363.

Odell, G. M., G. Oster, P. Alberch, and B. Burnside, 1981, "The mechanical basis of morphogenesis. I. Epithelial folding and invagination," *Dev. Biol.*, Vol. 85 (2), pp. 446–62.

Oster, G. F., J. D. Murray, and A. K. Harris, 1983, "Mechanical Aspects of Mesenchymal Morphogenesis," *J. Embryol. Exp. Res.*, Vol. 78, pp. 83–125.

Saad, Y., and M. H. Schultz, 1986, "GMRES: A generalized minimum residual algorithm for solving nonsymmetric linear systems," *SIAM J. Sci. Stat. Comp.*, Vol. 7, pp. 856–869.

Sangani, A. S., and C. Yao, 1988, "Transport Processes in Random Arrays of Cylinders. II. Viscous Flow," *Physics of Fluids*, Vol. 31 (9), pp. 2435–2444.

Scherer, G. W., 1989a, "Measurement of permeability—I. Theory," *J. Non-Crystalline Solids*, Vol. 113, pp. 107–118.

Scherer, G. W., 1989b, "Mechanics of syneresis—I. Theory," *J. Non-Crystalline Solids*, Vol. 108, pp. 18–27.

Schwartz, M., P. H. Leo, and J. L. Lewis, 1994, "A Microstructural Model of Articular Cartilage," *J. Biomech.*, Vol. 27 (7), pp. 865–873.

Sherratt, J. A., and J. Lewis, 1993, "Stress-induced alignment of actin filaments and the mechanics of cytogel," *Bull. Math. Biol.*, Vol. 55 (3), pp. 637–654.

Simon, B. R., and M. A. Gaballa, 1988, "Finite Strain, Poroelastic Finite Element Models for Large Arterial Cross Sections," in: *Computational Methods in Bioengineering*, Spilker, R. L., and Simon, B. R., eds., ASME, New York, pp. 325–333.

Stopak, D., and A. K. Harris, 1982, "Connective tissue morphogenesis by fibroblast traction. I. Tissue culture observations," *Dev Biol.*, Vol. 90 (2), pp. 383–398.

Tranquillo, R. T., and V. H. Barocas, 1996, "A continuum model for the role of fibroblast contact guidance in wound contraction," in: *Dynamics of Cell and Tissue Motion*, Alt, W., A. Deutsch, and G. A. Dunn, eds., Birkhauser Verlag, Basel.

Tranquillo, R. T., M. A. Durrani, and A. G. Moon, 1992, "Tissue engineering science: consequences of cell traction force," *Cytotechnology*, Vol. 10, pp. 225–250.

Tranquillo, R. T., T. S. Girton, B. A. Bromberek, T. G. Triebes, and D. L. Mooradian, 1996, "Magnetically-oriented tissue-equivalent tubes: application to a circumferentially-oriented media-equivalent," *Biomaterials*, Vol. 17, p. 349.

Weinberg, C. B., and E. Bell, 1986, "A blood vessel model constructed from collagen and cultured vascular cells," *Science*, Vol. 231 (4736), pp. 397–400.

Wilkins, L. M., S. R. Watson, S. J. Prosky, S. F. Meunier, and N. L. Parenteau, 1994, "Development of a bilayered living skin construct for clinical applications," *Biotech. and Bioeng.*, Vol. 43 (8), pp. 747–756.

Yannas, I. V., J. F. Burke, D. P. Orgill, and E. M. Skrabut, 1982, "Wound tissue can utilize a polymeric template to synthesize a functional extension of skin," *Science*, Vol. 215 (4529), pp. 174–176.

APPENDIX

We demonstrate here the derivation of the elements of $\mathbf{\Omega}_f$ from the deformation tensor $\mathbf{B}$. We begin by diagonalizing $\mathbf{B}$,

$$\hat{\mathbf{B}} = \mathbf{X}^{-1}\mathbf{B}\mathbf{X} = \begin{bmatrix} \beta_1 & & \\ & \beta_2 & \\ & & \beta_3 \end{bmatrix} \tag{A1}$$

where β's are the eigenvalues of $\mathbf{B}$, chosen so that $\beta_1 > \beta_2 > \beta_3 > 0$. (Since $\mathbf{B}$ is positive definite, all eigenvalues must be real and positive.) We treat only the case of three unequal eigenvalues here; if any two eigenvalues are equal, the analysis is simplified. We subsequently calculate the eigenvalues of $\mathbf{\Omega}_f$ in the transformed coordinate system, and then use the eigenvector matrix $\mathbf{X}$ to return to the original (r, θ, z) coordinates.

The normalization factor A is defined by

$$A = \int_0^{\pi/2}\int_0^{2\pi} \frac{r}{2\pi}\sqrt{\left(\frac{\partial r}{\partial \vartheta}\right)^2 + \left(\frac{\partial r}{\partial \alpha}\right)^2 \sin^2\alpha + r^2\sin^2\alpha}\, d\vartheta d\alpha$$

$$\approx \int_0^{\pi/2}\int_0^{2\pi} \frac{r^2(\alpha, \vartheta)\sin(\alpha)}{2\pi}\, d\vartheta d\alpha \tag{A2}$$

where r, α, and ϑ are as shown in Fig. A1, and the second expression is the small-strain approximation of the first. The ellipsoid is defined by

$$\frac{x^2}{\beta_3^2} + \frac{y^2}{\beta_2^2} + \frac{z^2}{\beta_1^2} = 1 \tag{A3}$$

where

$$x = r\sin\alpha\cos\vartheta, \quad y = r\sin\alpha\sin\vartheta, \quad z = r\cos\alpha$$

Combining these gives

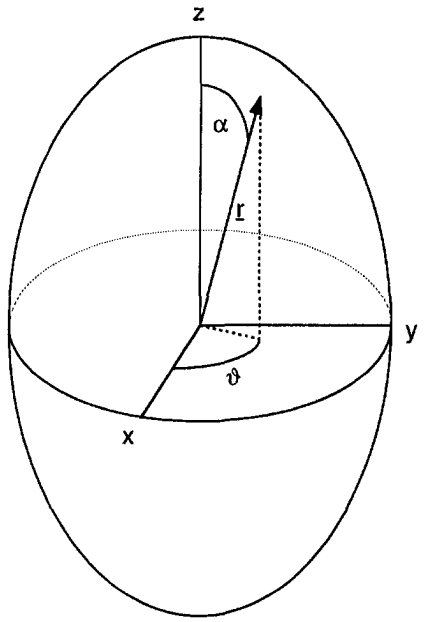

Fig. A1 Coordinates in calculation of Ω_f

$$A = \frac{\beta_1^2\beta_2^2\beta_3^2}{2\pi}\int_0^{\pi/2}\int_0^{2\pi}\frac{\sin\alpha\sqrt{\beta_1^4\beta_2^4\sin^2\alpha\cos^2\vartheta + \beta_1^4\beta_3^4\sin^2\alpha\sin^2\vartheta + \beta_2^4\beta_3^4\cos^2\alpha}}{(\beta_1^2\beta_2^2\sin^2\alpha\cos^2\vartheta + \beta_1^2\beta_3^2\sin^2\alpha\sin^2\vartheta + \beta_2^2\beta_3^2\cos^2\alpha)^2}\,d\vartheta d\alpha$$

$$\approx \frac{\beta_1^2\beta_2^2\beta_3^2}{2\pi}\int_0^{\pi/2}\int_0^{2\pi}\frac{\sin\alpha}{\beta_1^2\beta_2^2\sin^2\alpha\cos^2\vartheta + \beta_1^2\beta_3^2\sin^2\alpha\sin^2\vartheta + \beta_2^2\beta_3^2\cos^2\alpha}\,d\vartheta d\alpha \qquad \text{(A4)}$$

The first (general) form for A cannot be evaluated in terms of standard functions, and it is therefore solved numerically using *Mathematica;* the numerical results are then stored in a lookup table for use in simulations involving large deformations. The small-strain form can be written in terms of an elliptic integral of the first kind, $F(\phi, k)$,

$$A \approx \frac{\beta_1\beta_2\beta_3}{\sqrt{\beta_1^2 - \beta_3^2}}F(\phi, k) \qquad \text{(A5)}$$

where

$$\phi = \tan^{-1}\sqrt{\frac{\beta_1^2 - \beta_3^2}{\beta_3^2}}, \quad k = \sqrt{\frac{\beta_1^2 - \beta_2^2}{\beta_1^2 - \beta_3^2}}$$

and

$$F(\phi, k) \equiv \int_0^{\phi}\frac{d\varphi}{\sqrt{1 - k^2\sin^2\varphi}}.$$

We are now prepared to calculate the eigenvalues of Ω_f. The vector $\mathbf{r}$ in Eq. (13) can be written

$$\mathbf{r} = [\cos\alpha \quad \sin\alpha\sin\vartheta \quad \sin\alpha\cos\vartheta]^T$$

so that

$$\mathbf{r}\otimes\mathbf{r} = \begin{bmatrix} \cos^2\alpha & \sin\alpha\cos\alpha\sin\vartheta & \sin\alpha\cos\alpha\cos\vartheta \\ \sin\alpha\cos\alpha\sin\vartheta & \sin^2\alpha\sin^2\vartheta & \sin^2\alpha\sin\vartheta\cos\vartheta \\ \sin\alpha\cos\alpha\cos\vartheta & \sin^2\alpha\sin\vartheta\cos\vartheta & \sin^2\alpha\cos^2\vartheta \end{bmatrix}.$$

The off-diagonal terms vanish by symmetry of ϑ. Again, the general forms can only be calculated numerically, but the small-strain forms can be expressed in terms of elliptic integrals:

$$\hat{\Omega}_{f,11} \approx \frac{3\beta_1^3\beta_2\beta_3}{A(\beta_1^2 - \beta_2^2)\sqrt{\beta_1^2 - \beta_3^2}}[F(\phi, k) - E(\phi, k)] \qquad \text{(A6)}$$

where ϕ and k are defined as above and

$$E(\phi, k) \equiv \int_0^{\phi}\sqrt{1 - k^2\sin^2\varphi}\,d\varphi$$

Substituting the expression for A into Eq. (A6) gives the desired result:

$$\hat{\Omega}_{f,11} \approx \frac{3\beta_1^2}{\beta_1^2 - \beta_2^2}\left[1 - \frac{E(\phi, k)}{F(\phi, k)}\right] \qquad \text{(A7)}$$

Similarly,

$$\hat{\Omega}_{f,33} \approx \frac{3\beta_3^2}{\beta_2^2 - \beta_3^2}\left[\frac{\frac{\beta_2}{\beta_1}\sqrt{\frac{\beta_1^2 - \beta_3^2}{\beta_3^2}} - E(\phi, k)}{F(\phi, k)}\right] \qquad \text{(A8)}$$

and we simply write $\hat{\Omega}_{f,22} = 3 - (\hat{\Omega}_{f,11} + \hat{\Omega}_{f,33})$. As mentioned above, once Ω_f has been determined in the frame of the eigenvectors, it is transformed back to (r, θ, z) space for use in Eqs. (7) and (8).